Comparative engraftment and clonality of macaque HSPCs expanded on human umbilical vein endothelial cells versus non-expanded cells

Sandeep K. Srivastava,[1] Lauren L. Truitt,[2] Chuanfeng Wu,[2] Adam Glaser,[2] Daniel J. Nolan,[3] Michael Ginsberg,[3] Diego A. Espinoza,[2] Samson Koelle,[2,4] Idalia M. Yabe,[2] Kyung-Rok Yu,[2,5] Sogun Hong,[2] Stephanie Sellers,[2] Allen Krouse,[2] Aylin Bonifacino,[2] Mark Metzger,[2] Pradeep K. Dagur,[6] Robert E. Donahue,[2] Cynthia E. Dunbar,[2] and Sandhya R. Panch[1]

[1]Center for Cellular Engineering, Clinical Center, National Institutes of Health, Bethesda, MD 20892, USA; [2]Translational Stem Cell Biology Branch, National Heart, Lung and Blood Institute, National Institutes of Health, Bethesda, MD 20892, USA; [3]Angiocrine Bioscience, La Jolla, CA, USA; [4]Department of Statistics, University of Washington, Seattle, WA 98195, USA; [5]Department of Agricultural Biotechnology and Research Institute of Agriculture and Life Sciences, Seoul National University, Seoul 00826, Republic of Korea; [6]Flow Cytometry Core, National Heart, Lung and Blood Institute, National Institutes of Health, Bethesda, MD 20892, USA

Ex vivo hematopoietic stem and progenitor cell (HSPC) expansion platforms are under active development, designed to increase HSPC numbers and thus engraftment ability of allogeneic cord blood grafts or autologous HSPCs for gene therapies. Murine and *in vitro* models have not correlated well with clinical outcomes of HSPC expansion, emphasizing the need for relevant pre-clinical models. Our rhesus macaque HSPC competitive autologous transplantation model utilizing genetically barcoded HSPC allows direct analysis of the relative short and long-term engraftment ability of lentivirally transduced HSPCs, along with additional critical characteristics such as HSPC clonal diversity and lineage bias. We investigated the impact of *ex vivo* expansion of macaque HSPCs on the engineered endothelial cell line (E-HUVECs) platform regarding safety, engraftment of transduced and E-HUVEC-expanded HSPC over time compared to non-expanded HSPC for up to 51 months post-transplantation, and both clonal diversity and lineage distribution of output from each engrafted cell source. Short and long-term engraftment were comparable for E-HUVEC expanded and the non-expanded HSPCs in both animals, despite extensive proliferation of CD34+ cells during 8 days of *ex vivo* culture for the E-HUVEC HSPCs, and optimization of harvesting and infusion of HSPCs cocultured on E-HUVEC in the second animal. Long-term hematopoietic output from both E-HUVEC expanded and unexpanded HSPCs was highly polyclonal and multilineage. Overall, the comparable HSPC kinetics of macaques to humans, the ability to study post-transplant clonal patterns, and simultaneous multi-arm comparisons of grafts without the complication of interpreting allogeneic effects makes our model ideal to test *ex vivo* HSPC expansion platforms, particularly for gene therapy applications.

INTRODUCTION

The development of *ex vivo* hematopoietic stem cell expansion platforms could be of significant value in cord blood transplantation, producing higher numbers of engrafting cells and thus accelerated and more robust recovery, and in autologous hematopoietic stem and progenitor cell (HSPC) gene therapies, increasing the dose of transduced or edited cells and decreasing the need for fully myeloablative toxic conditioning therapies. Early attempts to expand HSPCs via *ex vivo* culture with various combinations of hematopoietic cytokines generally resulted in impaired or at best maintained short- and long-term engraftment, despite many-fold increases in HSPC cell numbers transplanted, demonstrating that expansion of HSPC numbers, or even phenotypically defined, putatively more primitive HSPCs, does not always correlate with improved functional engraftment.[1–3] Hence, recent protocols aimed at expanding primitive hematopoietic cells have added small molecules and/or adjuvant supportive cells or matrix compounds together with cytokines during *ex vivo* expansion, in an attempt to provide a more normal marrow microenvironment better preserving self-renewal and engraftment capabilities.[4–11]

To date, several hundred patients have been enrolled in allogeneic umbilical cord blood transplantation trials studying the safety and/or efficacy of various platforms for *ex vivo* expansion, with additional projected recruitment of many more in multiple ongoing phase I/II studies worldwide.[12] While *ex vivo* expanded human HSPCs have shown successful multi-lineage and long-term reconstitution in immune-deficient mice, these early phase clinical trials have failed to clearly demonstrate improved outcomes such as faster blood count

recovery or decreased complications of transplantation in patients. Most of these trials have utilized a dual umbilical cord HSPC design; with one cord *ex vivo* expanded and the non-expanded cord co-infused into the recipient. Some studies reported improved platelet and neutrophil recovery times mediated by the expanded cord. In most instances, however, the non-expanded cord generated more long-term steady-state hematopoietic output.[13] As such, murine models may misrepresent post-transplant engraftment in humans.

In addition, it has been challenging to interpret expanded versus non-expanded stem cell behavior in the context of three-party allogeneic graft-versus-host, host-versus-graft, and graft-versus-graft interactions following human allogeneic transplantation. While study design adaptations, such as adding back T cells from the expanded cord and better histocompatibility leukocyte antigen (HLA) matching, have helped control for these competing allogeneic effects, results have remained equivocal.[4] Thus, an autologous transplantation pre-clinical model may be better suited to evaluate relative engraftment kinetics and durability following various expansion approaches, independent of alloimmune factors.

Murine models have also sub-optimally addressed safety concerns seen with certain HSPC expansion techniques, particularly those combined with gene transfer vectors carrying a significant risk of insertional mutagenesis.[14] Clinically relevant large-animal models have better predicted these risks in humans.[15,16] Consequently, prior to clinical scale-up of any expansion platform for gene therapies or gene editing, a careful evaluation of *in vivo* hematopoietic clonal dynamics is critical to rule out any potential enhancement of genotoxicity due to *ex vivo* expansion stress.[17]

Over the last 2 decades, our group has utilized a rhesus macaque autologous myeloablative transplantation model to investigate hematopoiesis and optimize the safety and efficacy of gene and cell therapies. A competitive transplantation design and *ex vivo* lentiviral genetic tagging have allowed for the simultaneous *in vivo* comparison of multiple experimental arms of differentially manipulated HSPC fractions.[18,19] Recently, the gene tagging technique was further enhanced by the use of high diversity genetic barcodes within the lentiviral construct to facilitate highly quantitative interrogation of HSPC behavior at the clonal level.[20] We hypothesized that an autologous competitive transplantation model tracking contributions and clonality in rhesus macaques receiving barcoded CD34$^+$ HSPCs can serve as a clinically relevant platform to test novel expansion strategies.

Endothelial cells (ECs) play a central role in the bone marrow stromal microenvironment and act as a source for numerous hematopoietic growth factors. Preclinical studies have demonstrated significantly increased human cord blood CD34$^+$ cell expansion during co-culture with human umbilical vein endothelial cells (HUVECs).[21] Expansion of HSPCs was enhanced by adenoviral *E4ORF1* gene transduction of the HUVECs (E-HUVECs). This confers the ability of HUVECs to retain hematopoietic support functions in serum-free media for prolonged periods. These modified E-HUVECs are able to expand

CD34$^+$ cells capable of long-term stable reconstitution in immunodeficient mice.[22,23] Further, unlike small molecules, which are likely limited to single targets or pathways possibly resulting in biased differentiation, we hypothesized that niche-mimicking platforms (i.e., E-HUVEC co-culture platform) potentially target multiple pathways via the release of cytokines, for instance endothelial angiocrine factors critical for HSPC proliferation without loss of engraftment and self-renewal potential.[24–26] Because of this promising pre-clinical data, we evaluated the post-transplant safety and efficacy (engraftment and long-term repopulation potential) of E-HUVEC-co-cultured CD34$^+$ cells in our rhesus macaque competitive autologous transplantation model, allowing direct comparisons between expanded and non-expanded cells transduced with barcoded lentiviral vectors.

RESULTS

Rhesus macaque competitive transplantation study design and model optimization

We performed autologous transplantations in 2 rhesus macaques using mobilized peripheral blood HSPCs collected by leukapheresis. In the first animal (ZJ25), the study design included allocation of collected HSPCs into 3 parallel arms: E-HUVEC-expanded CD34$^+$ HSPCs with cytokine addition, RetroNectin (RN)-expanded CD34$^+$ HSPCs with cytokine addition, and non-expanded CD34$^+$ HSPCs. For each arm, an equal number of freshly purified CD34$^+$ HSPCs were transduced with a barcoded lentiviral vector library containing a murine stem cell virus (MSCV) viral promoter, a unique library ID for each arm, a highly diverse barcode library, and a green fluorescent protein (GFP) marker. The barcode library diversity for all barcoded lentivectors was ascertained to be sufficient for all transduced arms, with a greater than 95% chance that each unique barcode was present in only a single HSPC (Figure S1).

Then, 2 of the 3 HSPC fractions (E-HUVEC and RN-expanded) were expanded *ex vivo* for 8 days followed by cryopreservation. The third non-expanded HSPC fraction was cryopreserved immediately after transduction. All 3 cell fractions were then thawed and co-infused simultaneously into the animal as shown in Figure 1A and described in the Materials and methods section. Cryopreservation of all fractions was required to allow simultaneous transplantation of both expanded and non-expanded arms, as well as to model clinical studies, where cryopreservation of expanded grafts, particularly following genetic manipulation, is generally required to allow analysis of whether grafts fulfill required release characteristics

In order to enhance clinical relevance of the model and to eliminate potential experimental confounders, we made modifications in the protocol prior to autologous transplantation of the second animal (11021072) as highlighted in Table 1. The barcoded lentiviral vector used for transduction of ZJ25 HSPCs contained a strong (MSCV) viral promoter driving GFP marker protein expression. Following transplantation of this animal, our laboratory identified aberrant clonal hematopoiesis of the erythroid and myeloid lineages in a single rhesus macaque receiving HSPCs transduced with a lentiviral vector containing the MSCV promoter as part of a different study,[27] despite
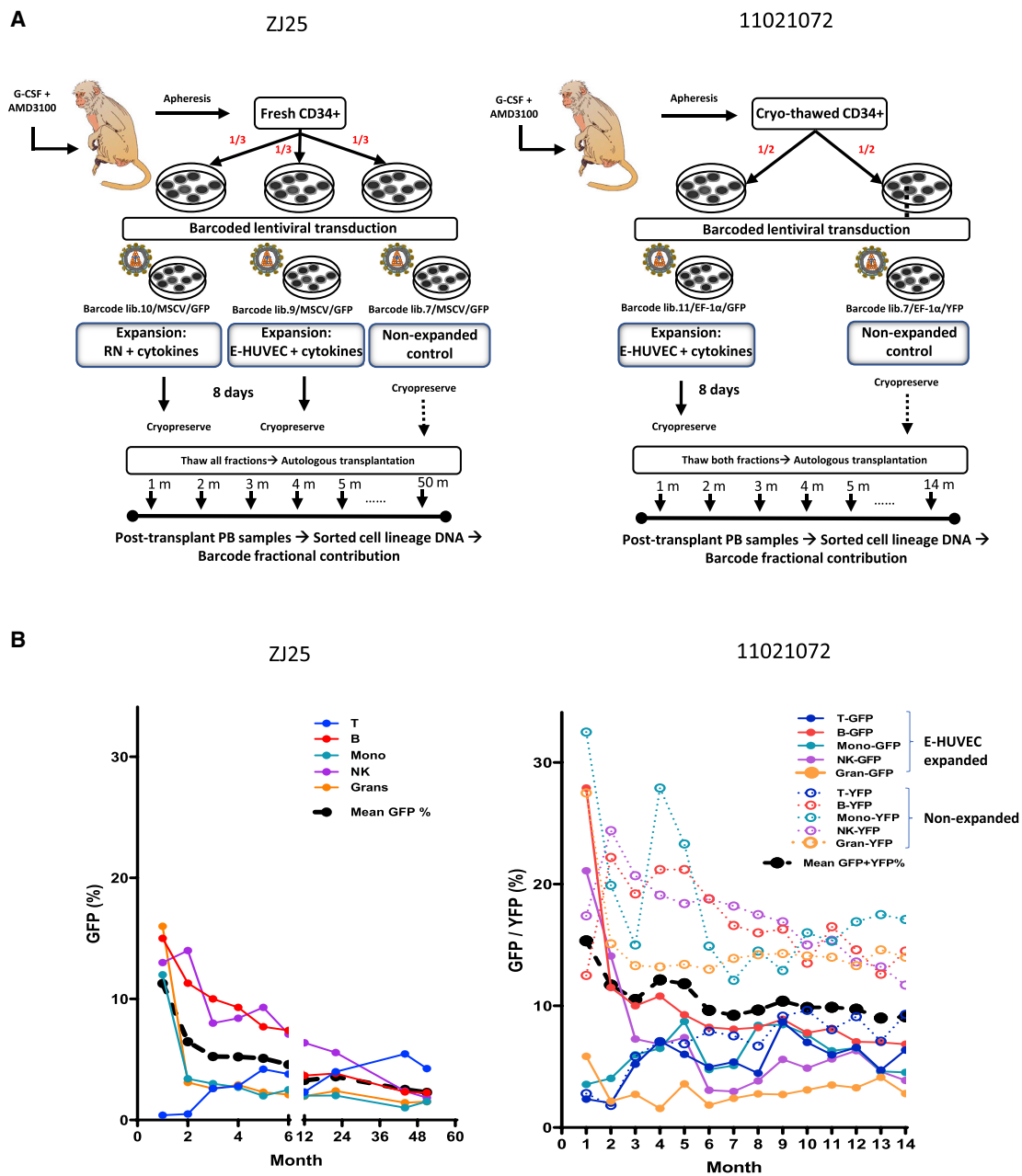
Figure 1. Study Design and Engraftment

(A) Animal-specific transplantation and *ex vivo* expansion schema. Mobilized peripheral blood CD34$^+$ cells from animal ZJ25 were split into 3 equal aliquots and each fraction was transduced with barcoded lentiviral constructs containing an MSCV promoter, a GFP marker gene, and one of 3 unique library IDs. After transduction, the non-expanded fraction was cryopreserved and the 2 remaining fractions were expanded in flasks on E-HUVECs or on RetroNectin (RN) plus cytokines for 8 days, harvested from the flasks via mechanical scraping, and then cryopreserved. All 3 fractions were thawed, filtered, mixed together, and then infused into the myeloablated autologous macaque. For animal 11021072, CD34$^+$ cells were cryopreserved and then thawed prior to splitting into 2 aliquots for transduction with one of two lentiviral barcoded libraries containing an EF1-α promoter driving GFP or YFP. Following transduction, the non-expanded fraction was cryopreserved, and the 2nd fraction was expanded for 8 days on E-HUVEC in a Quantum bioreactor. Cells were harvested from the bioreactor via enzymatic digestion and cryopreserved, and then thawed for infusion into the autologous macaque. MSCV, murine stem cell virus promoter; EF1-α, elongation factor 1-α promoter; GFP, green fluorescent protein; YFP, yellow fluorescent protein; E-HUVECs, engineered human umbilical vein endothelial cells. (B) Engraftment of transduced cells post-transplantation. Fraction (%) of GFP$^+$ peripheral blood T cells, B cells, monocytes, NK cells, and granulocytes up to 50 months post-transplantation in animal ZJ25 and the fraction (%) of GFP$^+$ or YFP$^+$ cells up to 14 months in post-transplantation in animal 11021072.

Table 1. Model optimization prior to second macaque (11021072) transplantation

1	Mimic clinical study logistics	Modified HSPC cryopreservation
2	Safety enhancement	Lentiviral promoter change (MSCV to EF1-α)
3	Simplified comparative arms	2-arm instead of 3-arm competitive transplantation
4	Dual method assessment of competitive engraftment	Cell fraction tagging with unique fluorescent proteins in addition to gene barcoding
5	Enhanced clinical relevance	HSPC co-culture with E-HUVEC in bioreactors
6	Optimized cell harvest techniques to minimize cell damage and to enhance engraftment	Cell dissociation by trypsinization (instead of manual cell scraping)

prior studies tracking over 100,000 engrafting HSPC clones using this vector without clonal expansions.[28,29] Hence in animal 11021072, we utilized barcoded lentiviral vectors containing a predicted less genotoxic elongation factor 1-α (EF1-α) promoter[28] to minimize any effects of vector insertion on clonal HSPC dynamics post-transplantation. In addition, we inserted GFP versus yellow fluorescent protein (YFP) marker proteins, as well as separate library IDs into two lentiviral vector libraries, allowing direct comparisons of total engraftment output from each fraction via flow cytometry, as well as deep sequencing of the vector library ID. In animal 11021072, to optimize for clinical relevance and based on prior experience with RN-expanded expansion, this arm was not included (Figure 1A), allowing a simplified two arm design utilizing the GFP versus YFP vectors.

The other major alteration to animal 11021072 transduction and transplantation was the addition of the co-culture step within the Terumo BCT Quantum hollow fiber bioreactor, a clinically relevant co-culture device. In addition to the geometric configuration and the continuous media feeding characteristics of the bioreactor versus flask-based expansions, harvesting of HSPCs from the E-HUVEC support at the end of expansion in the bioreactor used for 11021072 was performed via enzymatic flushing, versus mechanical disruption then filtration in the flask-based approach used in ZJ25, which resulted in observed cell clumping and cell loss. 70% loss of the cellular material occurred in the E-HUVEC arm following the flask-based expansion between cell harvest and post cryopreservation thawing and filtering prior to infusion into animal ZJ25, compared to a 2% loss of material in the Quantum-based culture and harvesting procedure employed for expansion in animal 11021072 (Table 1). Of note also in animal 2, cellular material was de-clumped post-thaw with DNAase and heparin without filtration. In both animals, E-HUVEC made up approximately 20% of the final infusate.

Engraftment and infusional safety of E-HUVEC co-cultured macaque HSPCs

Following transplantation, engraftment and clonal contribution patterns for each lineage were mapped for over 50 months in ZJ25 and for 14 months in 11021072. The degree of *ex vivo* expansion of total

HSPC cell numbers and the resultant viable transplant cell doses are summarized in Table 2 and Figure S2. Despite identical calculated multiplicity of infection (MOI) for lentiviral vector dose used for transduction of cells in each arm for animal ZJ25, significant biologic variability was noted in the fraction of GFP⁺ cells following transduction, prior to transfer of these HSPCs to co-culture conditions for the 2 expansion arms (RN arm, GFP% = 29%; E-HUVEC arm, GFP% = 6.9%) and in the non-expanded arm (GFP = 28%). These differences in transduction efficiency between vector preparations have on occasion been observed in previous competitive transplantation experiments; however, results can be interpreted in the context of the initial transduction efficiencies. In animal 11021072, transduction efficiency measured at infusion was similar in the E-HUVEC and the non-expanded arms. In both animals, hematopoietic cell numbers expanded markedly during culture, 50- and 80-fold, respectively, compared to the non-expanded arm, with a lesser but still substantial increase of 6- to 16-fold in the number of CD34⁺ cells both animals in the E-HUVEC arms compared to the non-expanded arms. In ZJ25, increases in total number of harvested cells (TNCs) and CD34⁺ cell numbers were greater with E-HUVEC than with RN + cytokines (Figure S2).

No post-infusional toxicities were identified despite the co-infusion of residual E-HUVEC cells adhering to the harvested HSPCs. ZJ25 had E-HUVEC DNA detected in the peripheral blood by PCR at day 3 post-transplantation, but not thereafter. In 11021072, we could not detect E-HUVEC DNA in the blood at any time point (Figure S3A). Time to neutrophil and platelet engraftment in the animals that received E-HUVEC-expanded CD34⁺ cells was similar to historical control animals at our facility, despite targeting relatively low starting (pre-expansion) CD34⁺ cell doses/kg in the animals in this study (Figure S3B). Neither animal required transfusional support prior to engraftment (Figure S3B), in contrast to the need for transfusions in approximately half of historical animals receiving lentivirally transduced non-expanded cells following the same conditioning regimen. As with historically transplanted animals, in the animals that received E-HUVEC-expanded CD34⁺ cells, white blood cells (WBC), hemoglobin, and platelet counts remained stable throughout the post-transplant follow-up period (Figure S3C).

Multi-lineage engraftment with transduced cells was confirmed in both animals via flow cytometry for GFP- or YFP-expressing cells (Figure 1B). Similar to our historical experience,[20,29] both animals demonstrated higher levels of transgene-expressing granulocytes, B cells, monocytes, and natural killer (NK) cells in the immediate post-transplant period, reflecting higher transduction of short-term repopulating cells, followed by stabilization at lower levels by 4–6 months when contributions from long-term multilineage HSPCs begin to dominate. In addition, both animals showed a slow rise in GFP- or YFP-positive T cells, similar to slow recovery of T cell production in historical controls, given TBI damage to the thymus delaying production of new T cells, and presence of mature T cells through TBI conditioning. In ZJ25, cells derived from the non-expanded HSPC arm versus the two HSPC-expanded arms could not be distinguished via transgene expression, since all 3 lentiviral vector libraries expressed GFP.

Table 2. Transplantation information

ZJ25: Male; 4 years old; 6.9 kg	Non-expanded (control)	RN + cytokine expanded	E-HUVEC expanded
Starting CD34+ cell number (X10^6)	7	7	7
Final cell number after transduction or transduction-expansion (X10^6)	6.2	143	546[a]
	Product filtered (100 μm filter) to avoid infusion of large cell clumps		
Total viable cell number post thaw and filtration (X10^6)	6.2	100	164
Fraction of pre-cryopreservation	100%	70%	30%
CD34+ cells infused (X10^6)	5.8	88.0	98.9
Ratio of CD34+ cells infused (versus control non-expanded arm)	1	15	17
% GFP+ infused cells[b]	28%	29%	6.9%
Transduced CD34+ cells infused (X10^6)	1.6	25.5	6.8
Ratio of transduced CD34+ cells infused (versus control non-expanded arm)	1	16	4
11021072: Female; 7 years old; 6.5 kg	Non-expanded (control)		E-HUVEC expanded
Starting CD34+ cell number (X10^6)	15		15
Cell number after expansion (X10^6)	25		750[a]
	Product de-clumped post-thaw with DNAase and heparin, without filtration		
Total viable cell number post thaw (X10^6)	22		740
Fraction of original remaining	88%		98%
CD34+ cells infused (X10^6)	17.2		102.4
Ratio of transduced CD34+ cells infused (versus control non-expanded arm)	1		6
% transduced infused cells	49% (GFP)		48.7% (YFP)
Transduced CD34+ cells infused (X10^6)	8.4		49.9
Ratio of transduced CD34+ cells infused (versus control non-expanded arm)	1		6

[a]The total number of harvested cells (TNCs) included E-HUVEC endothelial cells, CD34+ cells, and differentiated hematopoietic cells. Approximately 20% of viable TNCs were E-HUVECs as assessed by FACS.
[b]GFP% in the infused cells were calculated for individual fractions before the product was combined for infusion.

In 11021072, having utilized GFP- versus YFP-containing vectors to mark the two experimental arms, the source of cells could be assessed by flow cytometry. In this animal, the fraction of hematopoietic cells of all lineages originating from the E-HUVEC-expanded GFP-marked HSPCs were lower compared to those originating from YFP-marked non-expanded HSPCs, despite similar GFP and YFP transduction fractions in the infused expanded and non-expanded grafts, and 6-fold more CD34+ cells present in the expanded graft (Figure 1B). Transduced engrafted cells of all lineages were observed to originate from the E-HUVEC-expanded and the non-expanded arms throughout follow-up, albeit at low levels in ZJ25 (Figure 1B).

Clonal contributions and dynamics from E-HUVEC-expanded and non-expanded HSPCs

Barcode deep sequencing analysis and library ID retrieval demonstrated long-term contributions from transduced HSPCs in all lineages originating from both the E-HUVEC and non-expanded arms in ZJ25 and 11021072. Compared to the other lineages, a 3- to

4-month lag period was identified in appearance of the transduced T cell clonal fraction in both animals but was no different in pattern comparing E-HUVEC-expanded and non-expanded arms (Figure 2A). As noted above, this delayed T lineage recovery pattern was similar to results in with other age-matched animals transplanted using barcoded, non-expanded CD34+ cells at our facility.[20,29]

In both animals, shared barcodes (representing individual HSPC clones) retrieved from the various blood lineages were used as a surrogate for determining hierarchical relationships between these lineages. Of the thousands of barcodes retrieved, we focused on the top 20 highest contributing barcodes in each of the lineage sorted samples over time and plotted these data as heatmaps for the E-HUVEC-expanded and non-expanded arms in each animal (Figure 2A). Similar to post-transplant clonal dynamics demonstrated in patients with immune deficiencies undergoing gene therapies and our prior studies in macaqes,[29,30] short-term, biased uni-lineage clones contributed to T, B, monocyte, NK, and granulocyte outputs in the first 1–

A

ZJ25

11021072

B

ZJ25

11021072
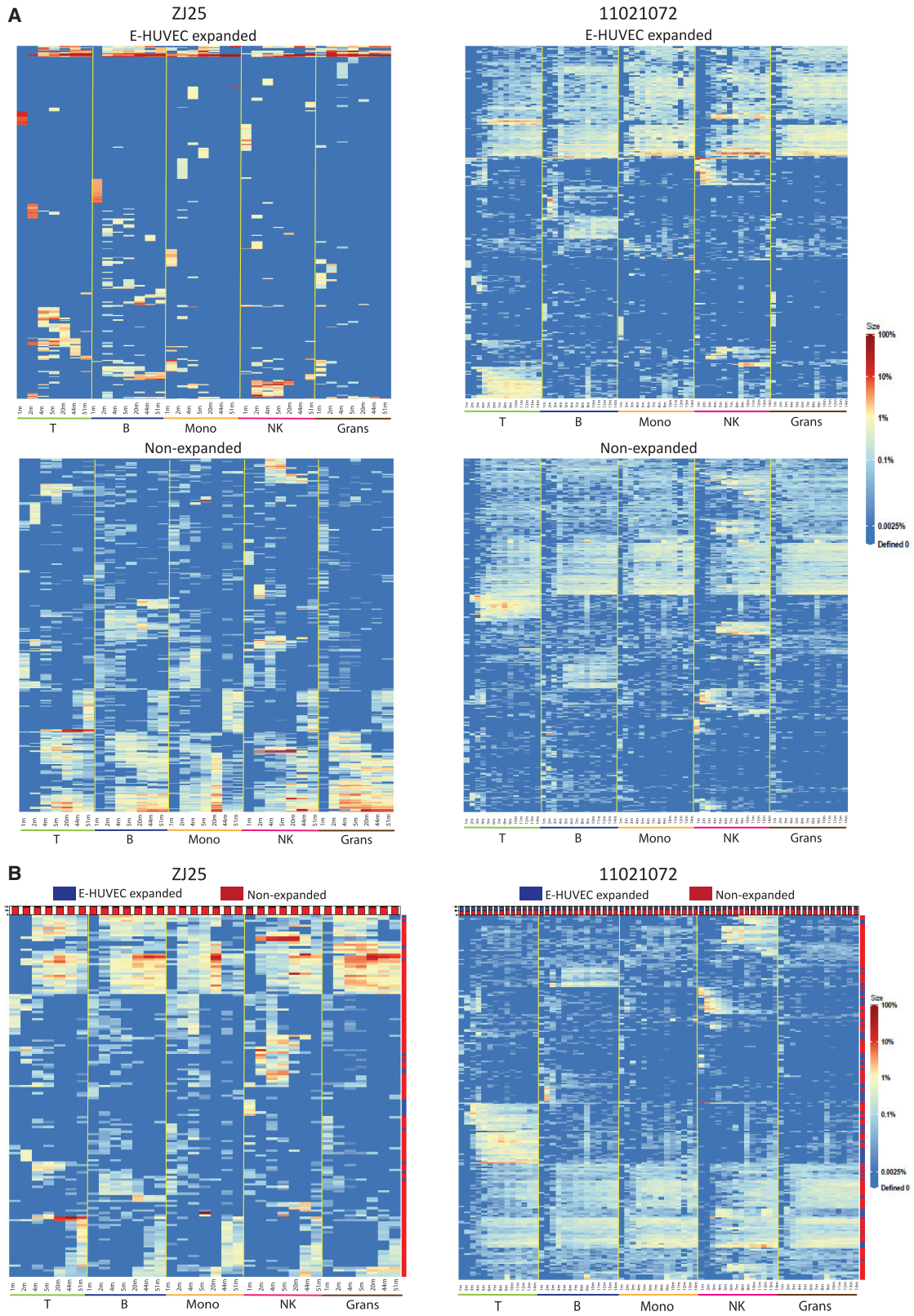
(legend on next page)

3 months. These were supplanted over time by multi-lineage clones, initially myeloid-restricted, and then by stable myeloid-B-T multi-lineage long-term repopulating clones. As reflected in the plots of pairwise Pearson correlations reflecting all clones, as well as heatmaps focused on the largest clones, regrouped as lineages within each time point (Figures S4A and S5A), in both animals the emergence of multi-potent clones was similar from control and E-HUVEC arms, i.e., at 3–4 months post-transplant, with initial engraftment supported by uni and bi-lineage clones. Further, as reported for other barcoded animals,[20,31] both T cells and mature NK cells demonstrated a restricted set of expanded clones originating from both arms, likely resulting from peripheral expansions of mature T and NK cells potentially in response to viral reactivation or other environmental cues, as detailed in our prior macaque studies, and prior human gene therapy analyses.[31–35] Similar clonal patterns were also observed in the RN + cytokines arm in ZJ25 (Figure S5B). Direct comparisons using a combined heatmap of the expanded and non-expanded HSPC barcodes/clones (Figure 2B) showed that clonal distributions and clonal dynamics were similar in E-HUVEC and non-expanded arms in both animals.

In the bone marrow, as previously demonstrated,[36] marked geographic segregation of CD34+ HSPCs from the left and right side was observed at 4 months in both animals in the E-HUVEC expanded and control arms (Figure S4B). Repeat bone marrow samples obtained at 51 and 15 months in ZJ25 and 11021072, respectively, demonstrated a complete (ZJ25, 51 months) or a partial (11021072, 15 months) mixing of clones without the appearance of abnormal clonal CD34+ cell populations. In summary, clonal reconstitution patterns derived from the E-HUVEC-expanded barcoded HSPCs were indistinguishable from those seen with non-expanded HSPCs.

Intermediate and long-term clonal stability in the expanded versus non-expanded HSPC

Clonal expansion was ruled out based on a look-back of the top contributing clones for each experimental arm at the point of longest follow-up, for each lineage (Figures 3; Figure S6). Even these large clones remained stable over time, with no evidence for aberrant ongoing clonal expansions of a particular clone or set of clones in ZJ25 through 50 months and in 11021072 through

14 months, respectively. In 11021072, similar to the relative levels of GFP versus YFP expressing peripheral blood (PB) cells detected by fluorescence-activated cell sorting (FACS), library ID retrieval demonstrated that engraftment in all lineages was somewhat better from the control versus the E-HUVEC-expanded fraction. Although the relative contribution from E-HUVEC-expanded cells was also lower in ZJ25, as demonstrated by library ID retrieval (Figure 3), the significantly lower transduction efficiency achieved in this arm (even prior to E-HUVEC co-culture) and much higher cell losses from the E-HUVEC fraction with non-enzymatic cell dissociation followed by cell scraping at harvest and cell filtration prior to transplant (Materials and methods; Table 1) compared to the non-expanded arm precluded definitive conclusions concerning relative engraftment potency in vivo in this animal. The level of engraftment originating from the E-HUVEC arm late following transplantation and the relative number of unique barcoded clones contributing to each experimental arm remained stable over time in both animals (Figure 4). In the RN + cytokine arm in ZJ25, a relative decrease in engraftment was observed over time, but with unique and cumulative barcode trends comparable to the E-HU-VEC-expanded and non-expanded arms (Figure S6).

DISCUSSION

Optimizing ex vivo hematopoietic stem cell expansion techniques to improve clinical outcomes after transplantation or gene therapies has become a major goal of hematopoiesis research over the past several decades. We report the development and utilization of a highly quantitative and sensitive pre-clinically relevant model to simultaneously compare the engraftment potential and in vivo behavior of ex vivo expanded HSPCs with their non-expanded counterparts, for the first time at a clonal level. Stem cell mobilization, collection, expansion and other manipulations, cryopreservation, and infusion parameters were designed to mimic autologous transplantation of transduced HSPCs in humans. The use of previously standardized protocols for non-human primate (NHP) RN flask coated expansions likely resulted in the loss of the majority of the most primitive HSPCs during filtering in animal ZJ25. Hematopoietic stem cell niches require direct contact and physical attachments between stem cells and ECs. For example, Jagged-2 signaling has been shown to be a necessary angiocrine factor to expand HSPCs in mice and requires intimate cell:cell contact.[25]

Figure 2. Heatmaps illustrating lineage contributions of top contributing clones

(A) Heatmaps representing fractional abundance of the highest-contributing clones defined as the top 20 highest-contributing barcodes in at least one of the samples, mapped over all samples for each animal, independently for each of the experimental arms (E-HUVEC-expanded versus non-expanded). Each row is a unique barcode and indicates that the barcode is one of the top 20 in one of the samples included and each column is a time point in months for lineages purified from peripheral blood samples, i.e., T, B, Mono (monocytes), NK cells, and grans (granulocytes). The barcodes are organized by unsupervised hierarchical clustering of the Euclidean distance between barcodes' log fractional abundances in the samples. Clones are clustered along the y axis to place similar clones next to each other. The relative contribution shown as a red-to-blue gradient, representing high contribution to no contribution, respectively, as shown in the legend. (B) Combined heatmap showing fractional abundance of clonal contributions from both E-HUVEC-expanded and non-expanded arms in animals ZJ25 and 11021072. Each vertical column represents a sample and each horizontal row a unique barcode. Bar graphs above each column show the total fractional contributions of the E-HUVEC-expanded (blue) and the non-expanded (red) arms for each lineage at each time point, considering the total contributions of each library across all relevant barcodes. The blue-red longitudinal bar on the right demonstrates the library of the corresponding barcode for each horizontal row. Due to the maintenance of unsupervised hierarchical clustering of barcodes, this bar also illustrates the overall similar kinetic and lineage characteristics of clones in the HUVEC-expanded versus non-expanded arms.

A

E-HUVEC expanded top 20 barcodes   E-HUVEC expanded other clones

Non-expanded top 20 barcodes   Non-expanded other clones
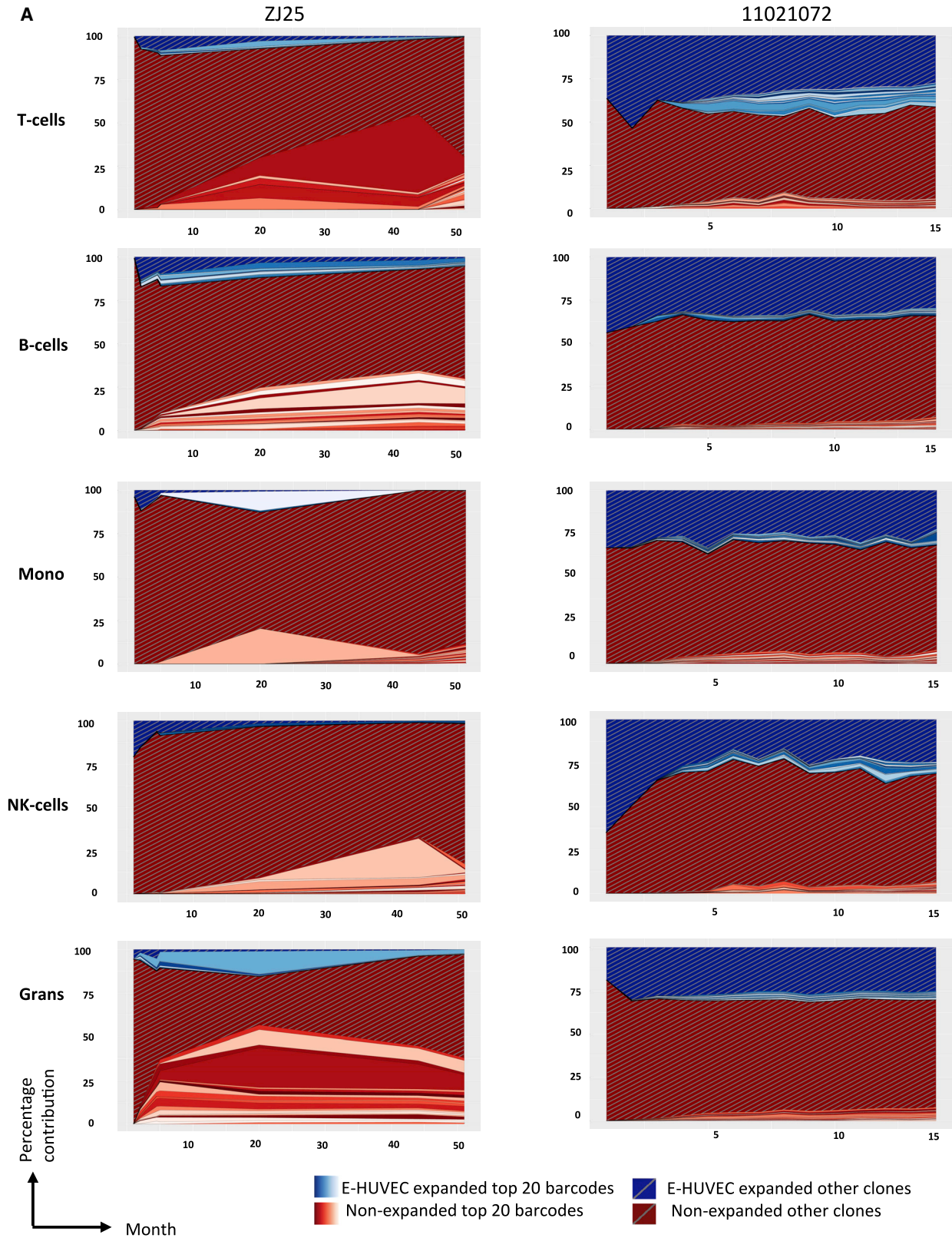
(legend on next page)

The more advanced clinical grade co-culture and harvest with the Quantum bioreactor used for animal 11021072 likely dissociated the EC:HSPC interaction more effectively, preventing any retention of the most primitive hematopoietic cells in the filter.

With E-HUVECs as feeder cell layers for HSPC expansion, we were able to demonstrate the safety and feasibility of expanding cells using this platform in our rhesus macaques. The competitive repopulation design of our study allowed direct assessment of the relative contributions of each transduced HSPC population to hematopoiesis over time and the pattern of clonal contributions from each cell source, using quantitative molecular library retrieval, with follow-up as long as 51 months. Another recent macaque study examined E-HUVEC HSPC expansion used a single-fraction, non-competitive transplantation design, precluding a head-to-head comparison of the experimental and "standard-of-care" arms.[37] However, the prior study also demonstrated safety, feasibility, and long-term stable engraftment of E-HUVEC-expanded HSPCs.

Long-term persistence of hematopoiesis derived from transduced HSPCs in the E-HUVEC-expanded cell fraction was equivalent or lower compared to the non-expanded arm, even in animal 11021072, with equivalent initial transduction efficiency in both arms, and 6-fold higher cell numbers and transduced cell numbers present following expansion. These results provide some evidence to suggest that at least lentivirally transduced rhesus macaque long-term engrafting HSPCs are not significantly increased with E-HUVEC expansion. However, the impact of E-HUVEC expansion on the non-transduced HSPCs cannot be assumed to be identical. Lentiviral transduction has been shown to be associated with p53 activation, apoptosis, and impaired proliferation of human HSPCs in some *in vitro* and xenograft studies,[38] with the largest impact on short-term as compared to long-term HSCs. We did not observe a diminution in the fraction-transduced cells present *in vitro* over the course of macaque HSPC expansion; however, a negative impact on actual engrafting transduced HSCs could be greater. It is also possible that peripheral blood HSPCs demonstrated lower expansion and migration/homing capability on this platform than umbilical cord blood HSPCs, the focus of most prior *ex vivo* expansion studies.[39,40] Therefore, our results may not apply to allogeneic cord blood transplantation or other non-transduced HSPC clinical applications. An ongoing trial (NCT03483324) investigates the impact of E-HUVEC co-culture using a dual cord blood design.

The lack of expansion of transduced long-term (LT)-HSPC may also be attributable to potential suboptimal interactions between macaque HSPC and the xenogeneic E-HUVEC, with potential lack of cross-reactivity of cytokines secreted by the E-HUVECs and differences in cell-cell interactions. In our preliminary *ex vivo* experiments, we found that macaque HSPC expansions were numerically comparable to that of human HSPCs carried out concurrently using this platform (data not shown), but there could be differential impacts on LT-HSCs.

Infusion of endothelial cells themselves may improve HSPC homing and engraftment. Chute et al.[41] demonstrated how dosing endothelial cells can rescue 100% of a population of animals receiving an LD50 dose of radiation without any hematopoietic rescue dose. Poulos et al.[42] replicated Chute's findings with culturable E4 murine ECs and found systemic benefits to the recipient animals, including accelerated hematopoietic recovery. A prior macaque transplantation study delivered only HSPCs and E-HUVECs harvested following expansion culture and documented prompt engraftment and no persistence of E-HUVEC DNA detectable *in vivo*.[37] In the current study, the mixture of both non-expanded HSPCs together with the expanded HSPCs and E-HUVECs could have enhanced engraftment of the non-expanded HSPCs.

The kinetics of hematopoietic cellular reconstitution after transplantation and gene therapy was evaluated in human clinical trials recently.[30] These were found to be significantly different from steady-state hematopoiesis.[43,44] Transplantation and stem cell aging are known to derail self-renewal and regenerative potential of the hematopoietic compartment. Further, senescent cells and/or aged host stem cell niches impose a myeloid bias on proliferating stem cells. Additionally, accumulations in DNA mutations with age may increase the occurrence of clonal hematopoiesis.[45] The replicative stress of *ex vivo* HSPC expansion may accelerate senescence over and above the pressure wielded by transplantation itself.[46,47] In our study, compared to non-expanded co-transplanted controls, we did not notice a myeloid bias or any instances of clonal expansions in the E-HUVEC-co-cultured HSPC fraction. This is in contrast to our previous study, which demonstrated a delayed emergence of multipotent clones, as well as a myeloid bias in aged versus young macaques.[48] It is possible that the endothelial cells rejuvenated the *ex vivo* expanded macaque HSPCs, circumventing the development of exhausted or senescent phenotypes.[49]

Lentiviral gene therapy using adult HSPCs collected from mobilized peripheral blood or non-mobilized bone marrow is another area of active investigation wherein gene transduction enhancers and *ex vivo* stem cell expanders are studied. Agents including Prostaglandin E2 and UM171 result in enhanced transduction efficiency and primitive hematopoietic stem cell expansion, respectively.[50,51] While our study was not designed to identify differences in

Figure 3. Clonal stability of top contributing clones

Stacked area plots showing the percentage contribution of the largest 20 contributing clones in each lineage (T, B, Mono, NK, Grans) for each experimental arm at the time of longest follow-up (50 months for ZJ25 and 14 months for 11021072), tracked over all time points. Each of the top 20 clones is shown as a separate colored ribbon in the stack, with shades of red representative of the non-expanded arm and shades of blue showing clones from the E-HUVEC arm. Contributions from the other (non-top 20) clones for each experimental fraction are shown as the remaining single lined solid colors (red, non-expanded; blue, E-HUVEC expanded).
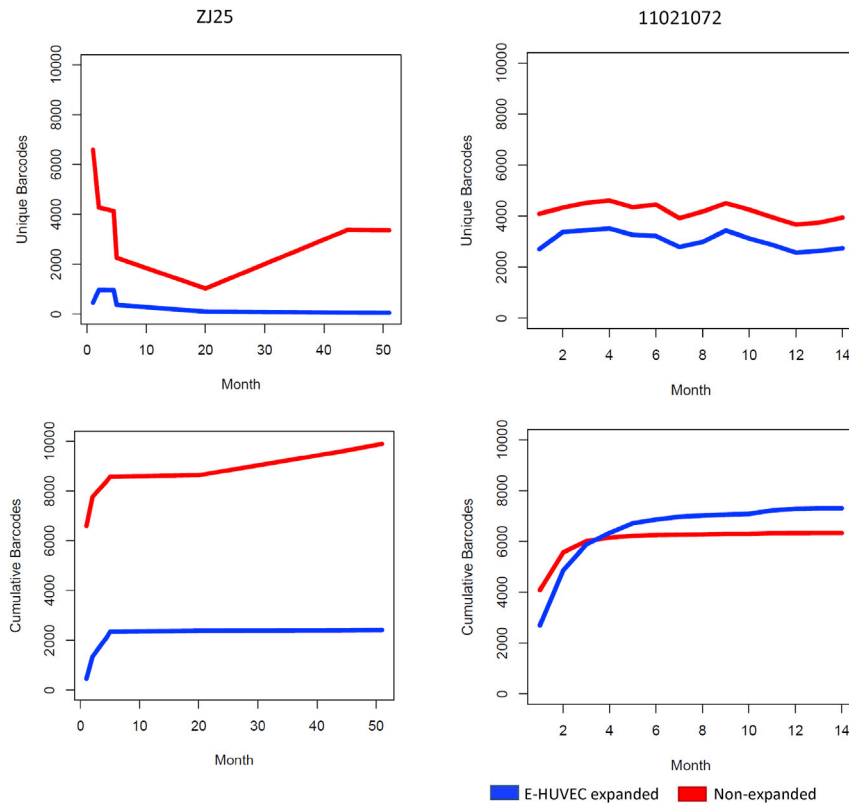
Figure 4. Post-transplant unique and cumulative barcodes

In ZJ25 and in 11021072 with the E-HUVEC-expanded and non-expanded arms in red and blue lines, respectively, with each unique barcode marking a single HSPC and its clonal progeny. The number of unique barcodes were retrieved from all lineages (T, B, monocytes, NK cells, and granulocytes) at a single time point for each experimental arm in both animals. The same barcode found contributing to more than one lineage was counted only once. The cumulative number of unique barcodes were retrieved for each experimental arm from all lineages combined (T, B, monocytes, NK cells, and granulocytes) over time in both animals. Clone numbers were calculated after applying a threshold of a clone achieving a fractional read abundance of at least 0.05% in at least 1 cell type at a minimum of at least 1 time point. The plateaus indicate highly sensitive capture of contributing clones.

transduction efficiency across the study arms (E-HUVEC arm transductions were also performed on RN-coated plates and then transferred for expansion on the feeder cell layers), it confirmed safety of this platform for the expansion of lentiviral-transduced cells. Given these findings, we recommend adapting our model for the preclinical testing of transduction enhancers as well. It also exemplifies the need for tailored protocols for each agent employed, even though this will make comparisons to historical controls more complicated.

In this study, despite modifications to our cell expansion/transplantation protocol prior to the second animal transplantation, safety and efficacy data described above were evaluable in both transplanted animals. Data from both animals demonstrated similar overall trends. The cumulative patterns described are particularly remarkable for the absence of abnormal clonal populations in both animals. Further, previously confirmed reports of robust data from clonal populations in non-human primates using the genetic barcoding technique even with low gene marking levels[52] precluded the need for a third resource-intense large-animal transplantation using the experimental parameters optimized in the course of our study.

In summary, our non-human primate model using competitively transplanted, gene-barcoded CD34+ cells represents a clinically relevant approach to study novel *ex vivo* stem cell expansion platforms and impact on *in vivo* hematopoietic reconstitution patterns over

time. Specifically, it is useful to assess immediate, intermediate, and long-term safety of these agents in a large-animal setting prior to clinical use in transplantation and/or gene therapy trials. With regard to the E-HUVEC platform, our model provides pre-clinical safety and efficacy data, showing sustained long-term contribution to post-transplant hematopoiesis with a normal clonal pattern, but no evidence for relative expansion of at least lentivirally transduced HSPCs compared to lentivirally transduced, non-expanded HSPCs. Further, prior to initiating resource-intensive clinical studies, which have minimally impacted long-term post-transplant outcomes thus far, it may be valuable to carry out cost-benefit analyses based on data generated from pre-clinical models like our non-human primate platform.

MATERIALS AND METHODS

Rhesus macaque HSPC collection, purification, and transplantation

All animal experiments were approved by the NHLBI Animal Care and Use Committee. Granulocyte- colony stimulating factor (G-CSF) (Amgen) 15 μg/kg/day for 5 days and AMD3100 (Sigma) 1 mg/kg on day 5 were administered subcutaneously to two rhesus macaques, followed by apheresis to collect mobilized peripheral blood mononuclear cells and enrichment for CD34+ HPSCs via immunoabsorption on Miltenyi cell separation columns as described.[53] Fresh (ZJ25) or cryopreserved-thawed (11021072) CD34+ cells were split into equal fractions and each was transduced with a separate barcoded lentiviral library capable of single cell clonal tracking within each fraction (see below). One fraction was cryopreserved immediately after transduction (non-expanded arm). The other fractions were expanded *ex vivo* for 8 days on E-HUVEC or in the presence of RN + cytokines (see below and Figure 1). Following myeloablative total-body irradiation of 500 rads X two on days −1 and 0, each of the

animals received an autologous intravenous infusion of a mixture of both thawed expanded and non-expanded cells.

DNA barcoding, retrieval, and analysis

High diversity 35-bp barcode libraries preceded by a 6-bp library ID were generated as previously described.[54] Barcoded libraries were cloned into lentiviral vectors containing either an internal human EF1-α promoter and a GFP marker, or a MSCV promoter/enhancer and either a GFP or YFP internal fluorescence marker. Retention of sufficient barcode diversity within each barcoded vector library was confirmed via Monte Carlo simulations, and vector libraries were only utilized for transplantation experiments if they were sufficiently diverse, with predicted >95% certainty that a single barcode would not be present in more than one HSPC following transduction.

For each animal, separate fractions of rhesus CD34-enriched HSPCs were each transduced with a distinct barcoded lentiviral vector library containing a unique library ID. Following autologous transplantation of expanded and non-expanded HSPCs, peripheral blood cells were isolated via density gradient separation over Ficoll, and specific lineages were purified via antibody staining and sorting on FACS Aria III flow cytometer (BD Biosciences, San Jose, CA, USA), using a gating schema shown in Figure S7A with the following antibodies: CD33, (Miltenyi Biotec, 130-098-864), CD3 (BD Biosciences, 563918), CD20 (BioLegend, 302313), CD14 (Miltenyi Biotec, 130-098-070), and NKG2A/C (Beckman Coulter, B10246). A post sort purity of >95% was confirmed in all sorted cell samples. DNA was extracted from each of the sorted samples using the DNeasy Blood and Tissue Kit (QIAGEN, Valencia, CA, USA), followed by amplification of the barcoded region via 28 cycles of PCR. Subsequently, samples were multiplexed for high-throughput sequencing on the Illumina HiSeq 2000 sequencer.[20]

For barcode data analysis, the sequencing output was de-multiplexed to obtain data from each sample using a custom python code, with quality control checks performed as previously described.[29] The fractional contribution of each barcode within each library ID (representing individual arms in the experiment) to a sample was then calculated from the ratio of the individual barcode's read number to the total number of valid barcodes reads in the sample. Stacked area plots were made using R studio (Integrated Development for RStudio, 2015, Boston, MA, USA; https://rstudio.com/). Heatmaps and correlation plots were produced using custom R code. Custom Python and R code are available at https://github.com/dunbarlabNIH. Prism 6.0 (GraphPad, La Jolla, CA, USA) was used to make dot plot diagrams and to calculate p values. Data on total sequenced reads and library-specific reads for both animals are presented in Tables S1 and S2.

Ex vivo expansion of rhesus HSPCs with E-HUVEC or RN + cytokines

Primary E-HUVECs (VeraVec PLATFORM, Angiocrine Bioscience) were thawed and grown at 37°C in the presence of 5% CO$_2$ for up to 3 passages to generate feeder cell layers. These cells were maintained in culture over the next 10 days in standard endothelial cell media as previously described.[55]

Fresh (animal ZJ25) or cryopreserved and then thawed (animal 11021072) rhesus macaque CD34$^+$ HSPCs were cultured overnight on RN-coated plates in X-VIVO 10 media (Lonza, Rockland, ME, USA) supplemented with 100 ng/mL each of human FLT3-L, stem cell factor (SCF), and thrombopoietin (Miltenyi Biotec) and 1% human albumin, and transduced with barcode-containing lentiviral vectors at a MOI of 25 in the presence of 4 μg/mL protamine sulfate (Sigma, St. Louis, MO, USA). Barcoded HSPCs were transferred 24 h later onto E-HUVEC feeder-cell flasks or onto fresh RN coated-flasks with cytokines (ZJ25) or a current Good manufacturing Practices (cGMP) compliant Quantum bioreactor (TerumoBCT) seeded with E-HUVECs (11021072). Cell fractions were expanded for 8 days with serial replating onto E-HUVECs based on cell density, maintaining an approximate ratio of 1:3 for HSPCs to E-HUVECs. In the RN + cytokine arm, cells were maintained at a concentration of 1 million cells/mL. For ZJ25, on day 8, cells present in the supernatant and adhered to E-HUVECs or RN + cytokines were harvested by non-enzymatic cell separation (enzyme-free dissociation buffer, GIBCO, 13150016) and manual scraping. For 11021072, on day 8 trypsin was added to the Quantum bioreactor for retrieval of HSPCs and E-HUVECs. All fractions were then cryopreserved.

Upon thaw of the HSPC, cell fractions, cell counts, and viability were assessed. Transduction efficiency (via GFP or YFP expression) and cellular phenotype were analyzed by flow cytometry following staining with the following antibodies: CD34 (BD Biosciences, 550761), CD45 (BD Biosciences, 561290), Efluor450 (e-Bioscience, 65-0863), CD144 (BD Biosciences, 565672), and CD31 (BD Biosciences, 563653) with gating as shown in Figure S7B. Of note, no attempt was made to separate E-HUVECs from HSPCs prior to infusion.

E-HUVEC detection in post-transplantation peripheral blood

Whole blood cells from before and following transplantation were red cell lysed, followed by DNA isolation and PCR assays using E4ORF1 gene-specific primers (Angiocrine Biosciences). Dilutions of DNA from E-HUVECs were used as positive controls.

SUPPLEMENTAL INFORMATION

Supplemental information can be found online at https://doi.org/10.1016/j.omtm.2021.02.009.

also supported by a materials transfer agreement with Angiocrine Biosciences and by the National Blood Foundation Grant awarded by the American Association of Blood Banks.

AUTHOR CONTRIBUTIONS

Contributions: S.R.P., S.K.S., C.W., D.J.N., M.G., and C.E.D. performed conceptualization of this work. D.A.E., S.K., and L.L.T., provided software; D.A.E., S.K., L.L.T., and P.K.D., conducted formal analysis. D.A.E. and L.L.T. performed visualization. S.R.P., S.K.S., I.M.Y., K.-R.Y., S.S., S. H., A.B., A.K., and M.M. conducted the investigations. C.E.D. and R.E.D. provided supervision. S.R.P., S.K.S., and C.E.D. wrote the manuscript.

DECLARATION OF INTEREST

REFERENCES

1. Metcalf, D. (2008). Hematopoietic cytokines. Blood *111*, 485–491.

2. Tisdale, J.F., Hanazono, Y., Sellers, S.E., Agricola, B.A., Metzger, M.E., Donahue, R.E., and Dunbar, C.E. (1998). Ex vivo expansion of genetically marked rhesus peripheral blood progenitor cells results in diminished long-term repopulating ability. Blood *92*, 1131–1141.

3. Zhang, C.C., and Lodish, H.F. (2008). Cytokines regulating hematopoietic stem cell function. Curr. Opin. Hematol. *15*, 307–311.

4. Wagner, J.E., Jr., Brunstein, C.G., Boitano, A.E., DeFor, T.E., McKenna, D., Sumstad, D., Blazar, B.R., Tolar, J., Le, C., Jones, J., et al. (2016). Phase I/II Trial of StemRegenin-1 Expanded Umbilical Cord Blood Hematopoietic Stem Cells Supports Testing as a Stand-Alone Graft. Cell Stem Cell *18*, 144–155.

5. Cutler, C., Multani, P., Robbins, D., Kim, H.T., Le, T., Hoggatt, J., Pelus, L.M., Desponts, C., Chen, Y.B., Rezner, B., et al. (2013). Prostaglandin-modulated umbilical cord blood hematopoietic stem cell transplantation. Blood *122*, 3074–3081.

6. North, T.E., Goessling, W., Walkley, C.R., Lengerke, C., Kopani, K.R., Lord, A.M., Weber, G.J., Bowman, T.V., Jang, I.H., Grosser, T., et al. (2007). Prostaglandin E2 regulates vertebrate haematopoietic stem cell homeostasis. Nature *447*, 1007–1011.

7. Horwitz, M.E., Chao, N.J., Rizzieri, D.A., Long, G.D., Sullivan, K.M., Gasparetto, C., Chute, J.P., Morris, A., McDonald, C., Waters-Pick, B., et al. (2014). Umbilical cord blood expansion with nicotinamide provides long-term multilineage engraftment. J. Clin. Invest. *124*, 3121–3128.

8. Delaney, C., Heimfeld, S., Brashem-Stein, C., Voorhies, H., Manger, R.L., and Bernstein, I.D. (2010). Notch-mediated expansion of human cord blood progenitor cells capable of rapid myeloid reconstitution. Nat. Med. *16*, 232–236.

9. de Lima, M., McNiece, I., Robinson, S.N., Munsell, M., Eapen, M., Horowitz, M., Alousi, A., Saliba, R., McMannis, J.D., Kaur, I., et al. (2012). Cord-blood engraftment with ex vivo mesenchymal-cell coculture. N. Engl. J. Med. *367*, 2305–2315.

10. Mehta, R.S., Saliba, R.M., Cao, K., Kaur, I., Rezvani, K., Chen, J., Olson, A., Parmar, S., Shah, N., Marin, D., et al. (2017). Ex Vivo Mesenchymal Precursor Cell-Expanded Cord Blood Transplantation after Reduced-Intensity Conditioning Regimens Improves Time to Neutrophil Recovery. Biol. Blood Marrow Transplant. *23*, 1359–1366.

11. Wilkinson, A.C., Ishida, R., Kikuchi, M., Sudo, K., Morita, M., Crisostomo, R.V., Yamamoto, R., Loh, K.M., Nakamura, Y., Watanabe, M., et al. (2019). Long-term ex vivo haematopoietic-stem-cell expansion allows nonconditioned transplantation. Nature *571*, 117–121.

12. Kiernan, J., Damien, P., Monaghan, M., Shorr, R., McIntyre, L., Fergusson, D., Tinmouth, A., and Allan, D. (2017). Clinical Studies of Ex Vivo Expansion to Accelerate Engraftment After Umbilical Cord Blood Transplantation: A Systematic Review. Transfus. Med. Rev. *31*, 173–182.

13. Lund, T.C., Boitano, A.E., Delaney, C.S., Shpall, E.J., and Wagner, J.E. (2015). Advances in umbilical cord blood manipulation-from niche to bedside. Nat. Rev. Clin. Oncol. *12*, 163–174.

14. Antonchuk, J., Sauvageau, G., and Humphries, R.K. (2002). HOXB4-induced expansion of adult hematopoietic stem cells ex vivo. Cell *109*, 39–45.

15. Larochelle, A., and Dunbar, C.E. (2008). HOXB4 and retroviral vectors: adding fuel to the fire. J. Clin. Invest. *118*, 1350–1353.

16. Zhang, X.B., Beard, B.C., Trobridge, G.D., Wood, B.L., Sale, G.E., Sud, R., Humphries, R.K., and Kiem, H.P. (2008). High incidence of leukemia in large animals after stem cell gene therapy with a HOXB4-expressing retroviral vector. J. Clin. Invest. *118*, 1502–1510.

17. Sellers, S., Gomes, T.J., Larochelle, A., Lopez, R., Adler, R., Krouse, A., Donahue, R.E., Childs, R.W., and Dunbar, C.E. (2010). Ex vivo expansion of retrovirally transduced primate CD34+ cells results in overrepresentation of clones with MDS1/EVI1 insertion sites in the myeloid lineage after transplantation. Mol. Ther. *18*, 1633–1639.

18. Donahue, R.E., and Dunbar, C.E. (2001). Update on the use of nonhuman primate models for preclinical testing of gene therapy approaches targeting hematopoietic cells. Hum. Gene Ther. *12*, 607–617.

19. Dunbar, C.E., Tisdale, J., Yu, J.M., Soma, T., Zujewski, J., Bodine, D., Sellers, S., Cowan, K., Donahue, R., and Emmons, R. (1997). Transduction of hematopoietic stem cells in humans and in nonhuman primates. Stem Cells *15* (*Suppl 1*), 135–139, discussion 139–140.

20. Wu, C., Li, B., Lu, R., Koelle, S.J., Yang, Y., Jares, A., Krouse, A.E., Metzger, M., Liang, F., Loré, K., et al. (2014). Clonal tracking of rhesus macaque hematopoiesis highlights a distinct lineage origin for natural killer cells. Cell Stem Cell *14*, 486–499.

21. Li, N., Eljaafari, A., Bensoussan, D., Wang, Y., Latger-Cannard, V., Serrurier, B., Boura, C., Kennel, A., Stoltz, J., and Feugier, P. (2006). Human umbilical vein endothelial cells increase ex vivo expansion of human CD34(+) PBPC through IL-6 secretion. Cytotherapy *8*, 335–342.

22. Seandel, M., Butler, J.M., Kobayashi, H., Hooper, A.T., White, I.A., Zhang, F., Vertes, E.L., Kobayashi, M., Zhang, Y., Shmelkov, S.V., et al. (2008). Generation of a functional and durable vascular niche by the adenoviral E4ORF1 gene. Proc. Natl. Acad. Sci. USA *105*, 19288–19293.

23. Butler, J.M., Gars, E.J., James, D.J., Nolan, D.J., Scandura, J.M., and Rafii, S. (2012). Development of a vascular niche platform for expansion of repopulating human cord blood stem and progenitor cells. Blood *120*, 1344–1347.

24. Li, Z., He, X.C., and Li, L. (2019). Hematopoietic stem cells: self-renewal and expansion. Curr. Opin. Hematol. *26*, 258–265.

25. Butler, J.M., Nolan, D.J., Vertes, E.L., Varnum-Finney, B., Kobayashi, H., Hooper, A.T., Seandel, M., Shido, K., White, I.A., Kobayashi, M., et al. (2010). Endothelial cells are essential for the self-renewal and repopulation of Notch-dependent hematopoietic stem cells. Cell Stem Cell *6*, 251–264.

26. Ding, L., Saunders, T.L., Enikolopov, G., and Morrison, S.J. (2012). Endothelial and perivascular cells maintain haematopoietic stem cells. Nature *481*, 457–462.

27. Espinoza, D.A., Fan, X., Yang, D., Cordes, S.F., Truitt, L.L., Calvo, K.R., Yabe, I.M., Demirci, S., Hope, K.J., Hong, S.G., et al. (2019). Aberrant Clonal Hematopoiesis following Lentiviral Vector Transduction of HSPCs in a Rhesus Macaque. Mol. Ther. *27*, 1074–1086.

28. Yabe, I.M., Truitt, L.L., Espinoza, D.A., Wu, C., Koelle, S., Panch, S., Corat, M.A.F., Winkler, T., Yu, K.R., Hong, S.G., et al. (2018). Barcoding of Macaque Hematopoietic Stem and Progenitor Cells: A Robust Platform to Assess Vector Genotoxicity. Mol. Ther. Methods Clin. Dev. *11*, 143–154.

29. Koelle, S.J., Espinoza, D.A., Wu, C., Xu, J., Lu, R., Li, B., Donahue, R.E., and Dunbar, C.E. (2017). Quantitative stability of hematopoietic stem and progenitor cell clonal output in rhesus macaques receiving transplants. Blood *129*, 1448–1457.

30. Scala, S., Basso-Ricci, L., Dionisio, F., Pellin, D., Giannelli, S., Salerio, F.A., Leonardelli, L., Cicalese, M.P., Ferrua, F., Aiuti, A., and Biasco, L. (2018). Dynamics of genetically engineered hematopoietic stem and progenitor cells after autologous transplantation in humans. Nat. Med. *24*, 1683–1690.

31. Wu, C., Espinoza, D.A., Koelle, S.J., Yang, D., Truitt, L., Schlums, H., Lafont, B.A., Davidson-Moncada, J.K., Lu, R., Kaur, A., et al. (2018). Clonal expansion and

compartmentalized maintenance of rhesus macaque NK cell subsets. Sci. Immunol. *3*, eaat9781.

32. Biasco, L., Scala, S., Basso Ricci, L., Dionisio, F., Baricordi, C., Calabria, A., Giannelli, S., Cieri, N., Barzaghi, F., Pajno, R., et al. (2015). In vivo tracking of T cells in humans unveils decade-long survival and activity of genetically modified T memory stem cells. Sci. Transl. Med. *7*, 273ra13.

33. Oliveira, G., Ruggiero, E., Stanghellini, M.T., Cieri, N., D'Agostino, M., Fronza, R., Lulay, C., Dionisio, F., Mastaglio, S., Greco, R., et al. (2015). Tracking genetically engineered lymphocytes long-term reveals the dynamics of T cell immunological memory. Sci. Transl. Med. *7*, 317ra198.

34. Truitt, L.L., Yang, D., Espinoza, D.A., Fan, X., Ram, D.R., Moström, M.J., Tran, D., Sprehe, L.M., Reeves, R.K., Donahue, R.E., et al. (2019). Impact of CMV Infection on Natural Killer Cell Clonal Repertoire in CMV-Naïve Rhesus Macaques. Front. Immunol. *10*, 2381.

35. Wu, C., Li, B., Lu, R., Koelle, S.J., Yang, Y., Jares, A., Krouse, A.E., Metzger, M., Liang, F., Loré, K., et al. (2014). Clonal tracking of rhesus macaque hematopoiesis highlights a distinct lineage origin for natural killer cells. Cell Stem Cell *14*, 486–499.

36. Wu, C., Espinoza, D.A., Koelle, S.J., Potter, E.L., Lu, R., Li, B., Yang, D., Fan, X., Donahue, R.E., Roederer, M., and Dunbar, C.E. (2018). Geographic clonal tracking in macaques provides insights into HSPC migration and differentiation. J. Exp. Med. *215*, 217–232.

37. Gori, J.L., Butler, J.M., Kunar, B., Poulos, M.G., Ginsberg, M., Nolan, D.J., Norgaard, Z.K., Adair, J.E., Rafii, S., and Kiem, H.P. (2017). Endothelial Cells Promote Expansion of Long-Term Engrafting Marrow Hematopoietic Stem and Progenitor Cells in Primates. Stem Cells Transl. Med. *6*, 864–876.

38. Piras, F., Riba, M., Petrillo, C., Lazarevic, D., Cuccovillo, I., Bartolaccini, S., Stupka, E., Gentner, B., Cittaro, D., Naldini, L., and Kajaste-Rudnitski, A. (2017). Lentiviral vectors escape innate sensing but trigger p53 in human hematopoietic stem and progenitor cells. EMBO Mol. Med. *9*, 1198–1211.

39. Tanavde, V.M., Malehorn, M.T., Lumkul, R., Gao, Z., Wingard, J., Garrett, E.S., and Civin, C.I. (2002). Human stem-progenitor cells from neonatal cord blood have greater hematopoietic expansion capacity than those from mobilized adult blood. Exp. Hematol. *30*, 816–823.

40. Voermans, C., Gerritsen, W.R., von dem Borne, A.E., and van der Schoot, C.E. (1999). Increased migration of cord blood-derived CD34+ cells, as compared to bone marrow and mobilized peripheral blood CD34+ cells across uncoated or fibronectin-coated filters. Exp. Hematol. *27*, 1806–1814.

41. Chute, J.P., Clark, W., Saini, A., Wells, M., and Harlan, D. (2002). Rescue of hematopoietic stem cells following high-dose radiation injury using ex vivo culture on endothelial monolayers. Mil. Med. *167* (2, Suppl), 74–77.

42. Poulos, M.G., Crowley, M.J.P., Gutkin, M.C., Ramalingam, P., Schachterle, W., Thomas, J.L., Elemento, O., and Butler, J.M. (2015). Vascular Platform to Define Hematopoietic Stem Cell Factors and Enhance Regenerative Hematopoiesis. Stem Cell Reports *5*, 881–894.

43. Sun, J., Ramos, A., Chapman, B., Johnnidis, J.B., Le, L., Ho, Y.J., Klein, A., Hofmann, O., and Camargo, F.D. (2014). Clonal dynamics of native haematopoiesis. Nature *514*, 322–327.

44. Busch, K., and Rodewald, H.R. (2016). Unperturbed vs. post-transplantation hematopoiesis: both in vivo but different. Curr. Opin. Hematol. *23*, 295–303.

45. de Haan, G., and Lazare, S.S. (2018). Aging of hematopoietic stem cells. Blood *131*, 479–487.

46. Allsopp, R.C., Morin, G.B., DePinho, R., Harley, C.B., and Weissman, I.L. (2003). Telomerase is required to slow telomere shortening and extend replicative lifespan of HSCs during serial transplantation. Blood *102*, 517–520.

47. Piacibello, W., Gammaitoni, L., and Pignochino, Y. (2005). Proliferative senescence in hematopoietic stem cells during ex-vivo expansion. Folia Histochem. Cytobiol. *43*, 197–202.

48. Yu, K.R., Espinoza, D.A., Wu, C., Truitt, L., Shin, T.H., Chen, S., Fan, X., Yabe, I.M., Panch, S., Hong, S.G., et al. (2018). The impact of aging on primate hematopoiesis as interrogated by clonal tracking. Blood *131*, 1195–1205.

49. Poulos, M.G., Ramalingam, P., Gutkin, M.C., Llanos, P., Gilleran, K., Rabbany, S.Y., and Butler, J.M. (2017). Endothelial transplantation rejuvenates aged hematopoietic stem cell function. J. Clin. Invest. *127*, 4163–4178.

50. Zonari, E., Desantis, G., Petrillo, C., Boccalatte, F.E., Lidonnici, M.R., Kajaste-Rudnitski, A., Aiuti, A., Ferrari, G., Naldini, L., and Gentner, B. (2017). Efficient Ex Vivo Engineering and Expansion of Highly Purified Human Hematopoietic Stem and Progenitor Cell Populations for Gene Therapy. Stem Cell Reports *8*, 977–990.

51. Masiuk, K.E., Zhang, R., Osborne, K., Hollis, R.P., Campo-Fernandez, B., and Kohn, D.B. (2019). PGE2 and Poloxamer Synperonic F108 Enhance Transduction of Human HSPCs with a β-Globin Lentiviral Vector. Mol. Ther. Methods Clin. Dev. *13*, 390–398.

52. Adair, J.E., Enstrom, M.R., Haworth, K.G., Schefter, L.E., Shahbazi, R., Humphrys, D.R., Porter, S., Tam, K., Porteus, M.H., and Kiem, H.P. (2020). DNA Barcoding in Nonhuman Primates Reveals Important Limitations in Retrovirus Integration Site Analysis. Mol. Ther. Methods Clin. Dev. *17*, 796–809.

53. Donahue, R.E., Kuramoto, K., and Dunbar, C.E. (2005). Large animal models for stem and progenitor cell analysis. Curr Protoc Immunol. *Chapter 22*. Unit 22A.1.

54. Lu, R., Neff, N.F., Quake, S.R., and Weissman, I.L. (2011). Tracking single hematopoietic stem cells in vivo using high-throughput sequencing in conjunction with viral genetic barcoding. Nat. Biotechnol. *29*, 928–933.

55. Gori, J.L., Butler, J.M., Chan, Y.Y., Chandrasekaran, D., Poulos, M.G., Ginsberg, M., Nolan, D.J., Elemento, O., Wood, B.L., Adair, J.E., et al. (2015). Vascular niche promotes hematopoietic multipotent progenitor formation from pluripotent stem cells. J. Clin. Invest. *125*, 1243–1254.